
DeepGO: Predicting protein functions from sequence and interactions using a deep ontology-aware classifier

Maxat Kulmanov¹, Mohammed Asif Khan¹, Robert Hoehndorf^{1, *},

**1 Computational Bioscience Research Center,
Computer, Electrical and Mathematical Sciences & Engineering Division,
King Abdullah University of Science and Technology,
4700 King Abdullah University of Science and Technology,
Thuwal 23955-6900, Kingdom of Saudi Arabia**

* robert.hoehndorf@kaust.edu.sa

Abstract

Motivation: A large number of protein sequences are becoming available through the application of novel high-throughput sequencing technologies. Experimental functional characterization of these proteins is time-consuming and expensive, and is often only done rigorously for few selected model organisms. Computational function prediction approaches have been suggested to fill this gap. The functions of proteins are classified using the Gene Ontology (GO), which contains over 40,000 classes. Additionally, proteins have multiple functions, making function prediction a large-scale, multi-class, multi-label problem.

Results: We have developed a novel method to predict protein function from sequence. We use deep learning to learn features from protein sequences as well as a cross-species protein-protein interaction network. Our approach specifically outputs information in the structure of the GO and utilizes the dependencies between GO classes as background information to construct a deep learning model. We evaluate our method using the standards established by the Computational Assessment of Function Annotation (CAFA) and demonstrate a significant improvement over baseline methods such as BLAST, with significant improvement for predicting cellular locations.

Availability and Implementation: Web server: <http://deepgo.bio2vec.net>, Source code: <https://github.com/bio-ontology-research-group/deepgo>

1 Introduction

Advances in sequencing technology have led to a large and rapidly increasing amount of genetic and protein sequences, and the amount is expected to increase further through sequencing of additional organisms as well as metagenomics. Although knowledge of protein sequences is useful for many applications, such as phylogenetics and evolutionary biology, understanding the behavior of biological systems additionally requires knowledge of the proteins' functions. Identifying protein functions is challenging and commonly requires *in vitro* or *in vivo* experiments [12], and it is obvious that experimental functional annotation of proteins will not scale with the amount of novel protein sequences becoming available.

One approach to address the challenge of identifying proteins' functions is the computational prediction of protein functions [22]. Function prediction can use several

sources of information, including protein-protein interactions [24], genetic interactions [12], evolutionary relations [14], protein structures and structure prediction methods [19], literature [28], or combinations of these [25]. These methods have been developed for many years, and their predictive performance is improving steadily [22].

There are several key challenges for protein function prediction methods. One of these is the complex relation between protein sequence, structure and function [2]; despite significant progress in the past years in protein structure prediction [20], it still requires large efforts to predict protein structure with sufficient quality to be useful in function prediction. Another challenge is the large and complex output space for any classification method. Protein functions are classified using the Gene Ontology (GO) [6] which contains over 40,000 functions and cellular locations. Additionally, the GO contains strong, formally defined relations between functions that need to be taken into account during function prediction to ensure that these predictions are consistent [22, 25]. The formal dependencies between classes in GO also lead to the situation where proteins are assigned to multiple function classes in GO, for different levels of abstraction. Furthermore, several proteins do not only have a single function but may be pleiotropic and have multiple different functions, making function prediction inherently a multi-label, multi-class problem. A final challenge is that proteins do not function in isolation. In particular higher-level physiological functions that go beyond simple molecular interactions, such as *apoptosis* or *regulation of heart rate*, will require other proteins and cannot usually be predicted by considering a single protein in isolation. Due to these challenges, it is also not obvious what kind of features should be used to predict the functions of a protein, and whether they can be generated efficiently for a large number of proteins.

Here, we present a novel method for predicting protein functions from protein sequence and known interactions. We combine two forms of representation learning based on multiple layers of neural networks to learn features that are useful for predicting protein functions, one method that learns features from protein sequence and another that learns representations of proteins based on their location in an interaction network. We then utilize these features in a novel deep neuro-symbolic model that is built to resemble the structure and dependencies between classes that exist within the GO, refine predictions and features on each level of GO, and ultimately optimize the performance of function prediction based on the performance over the whole ontology hierarchy.

We demonstrate that our model improves performance of function prediction over a BLAST baseline, and performs particularly well in predicting cellular locations of proteins. The main advantage of our approach is that it does not rely on manually crafted features but is entirely data-driven.

2 Materials and Methods

2.1 Datasets

For our experiments, we use the Gene Ontology (GO) [6], downloaded on 05 January 2016 from <http://geneontology.org/page/download-ontology> in OBO format. The version of GO has 44,683 classes of which 1,968 are obsolete. GO has three major branches, one for biological processes (BP), molecular functions (MF) and cellular components (CC), each containing 28,647, 10,161, and 3,907 classes, respectively.

We use SwissProt’s [9] reviewed and manually annotated protein sequences with GO annotations downloaded on 05 January 2016 from <http://www.uniprot.org/uniprot/>. The dataset contains 553,232 proteins, and 525,931 proteins have function annotations. Furthermore, we select proteins with annotations with experimental evidence code

(EXP, IDA, IPI, IMP, IGI, IEP, TAS and IC) and filter the proteins by maximum length of 1,002 ignoring proteins with ambiguous amino acid codes (B, O, J, U, X, Z) in their sequence. Our final dataset contains 60,710 proteins annotated with 27,760 classes (19,181 in BP, 6,221 in MF, and 2,358 in CC).

2.2 Training

We trained three models, one for each sub-ontology in GO. First, we propagate annotations using the GO ontology structure and randomly split proteins into a training set (80%) and testing set (20%). Due to computational limitations and the small number of annotations for very specific GO classes, we ranked GO classes by their number of annotations and selected the top 932 terms for BP, 589 terms for MF and 436 terms for the CC ontology. These cutoff values correspond to selecting only classes with the minimum number of annotations 250, 50, and 50, for BP, MF, and CC, respectively.

We create three binary label vectors for each protein sequence, one for each of the GO hierarchies. If a protein sequence is annotated with a GO class from our lists of selected classes, then we assign 1 to the term's position in the binary label vector and use it as positive sample for this term. Otherwise, we assign 0 and use it as negative sample. For training and testing, we use proteins which have been annotated with at least one GO term from the set of the GO terms for the model.

2.3 Data Representation

The input of our model is the amino acid (AA) sequence of a protein. Each protein is a character sequence composed of 20 unique AA codes. We generate trigrams of AA from the protein sequence. The trigrams can be represented as one-hot encoding vectors of length 8,000; however, the sparse nature of one-hot encodings only provides a limited generalization performance. To address this limitation, we use the notion of dense embeddings [7,17]. An embedding is a lookup table used for mapping each code in a vocabulary to a dense vector. Initially, we initialized the vectors randomly and then learn the actual vector-based representations as an additional layer in our network architecture during training. This approach allows us to learn meaningful vectors, i.e., vectors that resemble correlations within the data that can be utilized as features to predict protein functions. We have also performed experiments (on a smaller dataset) with one-hot encodings of AA trigrams, and found that dense representation performs better than one-hot encoding.

We built a vocabulary of unique AA trigrams where each trigram is represented by its 1-based index. Using this vocabulary, we encoded a sequence of length 1002 as a vector of 1000 indices. If the length of the sequence is less than 1002, we pad the vector with zeros. We ignore all the proteins with sequence length more than 1002. The first layer in the deep learning model is intended to learn embeddings where each index is mapped to a dense vector by referring to a lookup table, using an embedding size of 128 and therefore representing a protein sequence of length of 1002 as a matrix of 1000×128 .

2.4 Convolutional Neural Network

Convolutional Neural Networks (CNNs) are biologically inspired NN which try to mimic the receptive field of biological neuron. In CNNs, convolution operations are applied over the input layer to compute the output [8]. They exploit local correlation by enforcing local connections between neurons of adjacent layers, where each region of the input is connected to a neuron in the output. Having multiple convolution filters helps in learning multiple features and providing insights into multiple facets of the data. In

our work, we used 1-dimensional (1D) convolution over protein sequence data. The 1D convolution exploits sequential correlation. If we have an input $g(x) \in [1, l] \rightarrow \mathbb{R}$ and a kernel function $f(x) \in [1, k] \rightarrow \mathbb{R}$, the convolution $h(y)$ between $f(x)$ and $g(x)$ with stride d is defined as:

$$h(y) = \sum_{x=1}^k f(x) \cdot g(y \cdot d - x + c) \quad (1)$$

where $c = k - d + 1$ is an offset constant. The output $h_j(y)$ is obtained by a sum over i of the convolutions between $g_i(x)$ and $f_{ij}(x)$. The output vector h represents the feature map learned through convolution.

The resulting feature map will contain redundant information and is of significant size. Therefore, to reduce the feature space, redundant information is discarded through temporal max-pooling [11]. This operation selects the maximum value over a window of some length w . The features after convolution and the temporal pooling layer are intended to be higher level representation of protein sequences which can then be used as input to fully connected layers for classification.

For our experiments, we used one 1D Convolution layer with 32 filters of size 128 which are applied on the embedding matrix of each sequence, and a 1D max-pooling layer with pool length of 64 and stride of 32. Each filter is intended to learn a specific type of feature, and multiple filters may enable learning of different aspects of the underlying data. The output of the 1D max-pooling layer is a vector with length of 832.

2.5 Protein-protein interaction (PPI) network features

In addition to protein sequences, we use protein-protein interaction (PPI) networks for multiple species from the STRING database [26], filtered by confidence score of 300 and connected with orthology relations from the EggNOG database [18] by creating a symmetric *ortholog-of* edge for each orthology group. To further separate proteins by the orthology group to which they belong, we introduce a new orthology relation for each orthology group in eggNOG. In total, the network consists of 8,478,935 proteins, 190,649 edge types and 11,586,695,610 edges. Using this heterogeneous network, we generated knowledge graph embeddings of size 256 for each protein [4].

Since our model is based on UniProt protein identifiers, we mapped nodes in the network to UniProt identifiers using the identifier mapping provided by STRING. We mapped 6,960,395 proteins in UniProt to our network and the resulting knowledge graph embeddings. For the proteins with missing network representations, we assigned a vector of zeros. We combined the knowledge graph embeddings for the nodes with the output of the max-pooling layer of length 832 as a combined feature vector.

2.6 Hierarchical classification layout

Using a fully-connected layers for each class in GO, we created a hierarchical classification neural network model. We use only the subclass relations and create a small neural network for each class in our subset of selected terms. Each network consists of two fully-connected layers. The first layer has an output of 256 neurons with a Rectified linear unit (ReLU) activation function, and takes as an input the protein representation concatenated with a first layer outputs of the parent terms. The second layer has an output of a single neuron with a sigmoid activation function and takes as an input the output of the first layer. This layer is responsible for classifying the proteins for its term. To ensure consistent hierarchical classification, for each class which has children in GO, we created a merge layer which selects the maximum value of the classification layers of the term and its children. Finally, the output of the model is

the concatenation of classification layers of leaf nodes and the maximum layers of internal nodes. Figure 1 shows the architecture of our neural network model.

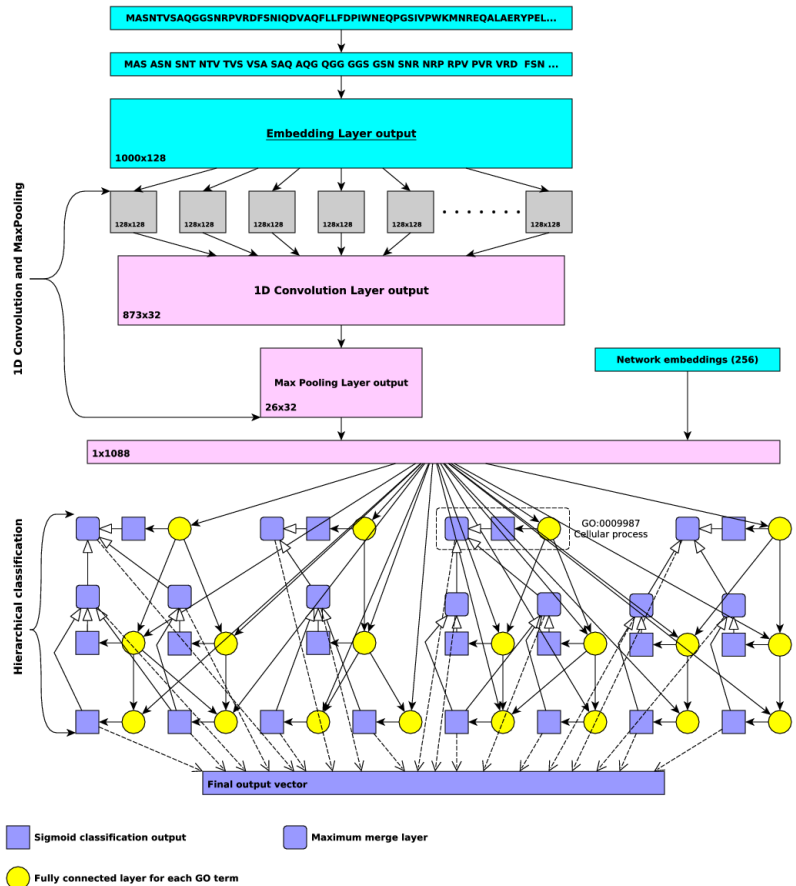


Figure 1. Convolutional Neural Network Architecture. 1) The input of the model is a list of integer indexes of trigrams generated from protein sequence and vector of size 256 for protein PPI network representation. The trigram indexes are passed to embedding layer which provides vector representations of size 128 for each trigram. The output of an embedding layer is a matrix of size 1000x128 on which we apply convolution and max-pooling. We merge the flattened output of the max-pooling layer with input PPI network representation which is then passed to hierarchical classification layers. 2) Hierarchical classification layers has a DAG structure of GO for is-a relations and for each GO term we created two fully-connected layers. First layer (yellow circle) has 256 neurons and it takes protein representation. Second layer (purple square) has 1 neuron and it is connected to the first layers and performs the classification for one GO term. Additionally, internal nodes in the graph have maximum merge layers (rounded purple square) which outputs the maximum value of all the children and second layer of the term. Finally, the output vector of the model is the concatenation of maximum merge layers of the internal nodes and classification layers of the leaf nodes.

2.7 Model implementation and optimization

In training, we minimize the multi-output binary cross entropy loss function using the Rmsprop optimizer [27] with a mini batch of size 128 and learning rate of 0.01. Initially,

the weights of our model are initialized according to a uniform distribution [16]. We fit our model with 80% of our training set and use the remaining 20% of the training set as a validation set. At the end of each training epoch, we monitor the convergence of the model on the validation set and keep the weights of the best performing model. To prevent over-fitting of the model, we use dropout layers as regularizers. We implement our model using the deep learning library Keras with TensorFlow [1] as a backend. To accelerate the training process, we use NVIDIA Pascal X GPUs. We manually tuned the following set of parameters: minibatch size, number of convolution filters, filter size, number of neurons in fully connected layer, and learning rate. Source code for our implementation is available at <https://github.com/bio-ontology-research-group/deepgo>.

2.8 BLAST baseline

We use the BLAST [5] sequence alignment method as a baseline to compare our model's performance. We use BLAST to find the most similar sequence in a database of experimentally annotated proteins for a query sequence and assign all its annotations to the query sequence. We create a database for each ontology with a proteins in our training set that have been annotated with at least one term from the ontology. For a proteins in our test set, we use the BLASTP program to obtain the protein with the highest alignment score from our training set and assign all its functional terms to the protein from our test set.

2.9 Evaluation

We evaluate our model performance with two measures [10] that are used in CAFA challenge [22]. The first measure is a protein centric maximum F-measure. Here, we compute F-measure for a threshold $t \in [0, 1]$ using the average precision for proteins for which we predict at least one term and average recall for all proteins. Then, we select the maximum F-measure of all thresholds. We compute the F_{max} measure using the following formulas:

$$pr_i(t) = \frac{\sum_f I(f \in P_i(t) \wedge f \in T_i)}{\sum_f I(f \in P_i(t))} \quad (2)$$

$$rc_i(t) = \frac{\sum_f I(f \in P_i(t) \wedge f \in T_i)}{\sum_f I(f \in T_i)} \quad (3)$$

$$AvgPr(t) = \frac{1}{m(t)} * \sum_{i=1}^{m(t)} pr_i(t) \quad (4)$$

$$AvgRc(t) = \frac{1}{n} * \sum_{i=1}^n rc_i(t) \quad (5)$$

$$F_{max} = \max_t \left\{ \frac{2 * AvgPr(t) * AvgRc(t)}{AvgPr(t) + AvgRc(t)} \right\} \quad (6)$$

In these measures, f is GO class, $P_i(t)$ is a set of predicted classes for a protein i using a threshold t , and T_i is a set of annotated classes for a protein i . Precision is averaged over the proteins where we at least predict one term and $m(t)$ is the total number of such proteins. n is a number of all proteins in a test set.

The second measure is a term-centric where for each term f we compute AUC of a ROC Curve of a sensitivity (or a recall) for a given false positive rate (1 - specificity). We compute sensitivity and specificity using the following formulas:

$$sn_f(t) = \frac{\sum_i I(f \in P_i(t) \wedge f \in T_i)}{\sum_i I(f \in T_i)} \quad (7)$$

$$sp_f(t) = \frac{\sum_i I(f \notin P_i(t) \wedge f \notin T_i)}{\sum_i I(f \notin T_i)} \quad (8)$$

Here, $P_i(t)$ is a set of predicted terms for a protein i using a threshold t and T_i is a set of annotated terms for a protein i . Additionally, we report a term-centric F_{max} measure where for each term f we compute the F-measure using threshold t and all proteins in our test set. Then, we take the maximum for all the thresholds.

$$pr_f(t) = \frac{\sum_i I(f \in P_i(t) \wedge f \in T_i)}{\sum_i I(f \in P_i(t))} \quad (9)$$

$$rc_f(t) = \frac{\sum_i I(f \in P_i(t) \wedge f \in T_i)}{\sum_i I(f \in T_i)} \quad (10)$$

$$F_{maxf} = \max_t \left\{ \frac{2 * pr_f(t) * rc_f(t)}{pr_f(t) + rc_f(t)} \right\} \quad (11)$$

3 Results

3.1 Feature learning and neuro-symbolic hierarchical classification

We build a machine learning model that aims to address three challenges in computational function prediction: learning features to represent a protein, predicting functions in a hierarchical output space with strong dependencies, and combining information from protein sequences with protein-protein interaction networks. The first part of our model learns a vector representation for a protein sequence which can be used as features to predict protein functions. The second part of the model aims to encode for the functional dependencies between classes in GO and optimizes classification accuracy over the hierarchical structure of GO at once instead of optimizing one model locally for each class. The intention is that this model can identify both explicit dependencies between classes in GO, as expressed by relations between classes encoded in the ontology, as well as implicit dependencies such as frequently co-occurring classes. While a single model over the entire GO would likely yield best results, due to the size of the GO, we independently train three models for each of GO’s three sub-ontologies, Molecular Function (MF), Biological Process (BP), and Cellular Component (CC), and focus exclusively on subclass relations between GO classes. We generate a series of fully connected layers, one for each class C in the GO. Each of these layers has exactly one connection to an output neuron, $Out(C)$, and, for each direct subclass D of C , a connection to another layer representing D . This architecture resembles the hierarchical structure of GO and the dependencies between its classes, ensures that discriminating features of each class can be learned hierarchically while taking into account the symbolic relations in GO. More generally, each dense layer of this ontology-structured neural network layout is intended to learn features that can discriminate between its subclasses and will pass these features on to the next layers. Figure 1 illustrates the basic architecture of our model.

We train three model in a supervised way (one model for each of the GO ontologies). For this purpose, we first split all proteins with manually curated GO annotations in SwissProt in a training set (80%) and an evaluation set (20%). We use the manually assigned GO functions of the proteins in the training set to train our models. The performance of each model is globally optimized over all the GO functions (within either the MF, BP, or CC hierarchy) through back-propagation. We then evaluate the performance of our model on the 20% of proteins not used for training, using the

evaluation metrics developed and employed in the CAFA challenge [22]. Table 1 shows the overall performance of our model and the comparison to using BLAST to assign functions. We find that our model, which relies only on protein sequences (DeepGOSeq), outperforms BLAST in predicting cellular locations, but does not achieve improved performance compared to BLAST in the MF and BP ontologies when evaluated either on the full set of GO functions or the subset used by our model.

3.2 Incorporating protein networks

The majority of functions and biological processes in GO require multiple proteins to be performed. One source of information for proteins acting together can be obtained from protein-protein interaction networks. By adding information about protein-protein interactions, we planned to improve our model’s performance, in particular for prediction of associations to biological processes which usually require more than one protein to be performed. We encode protein-protein interactions as a multi-species knowledge graph of interacting proteins in which proteins within a species are linked through *interacts-with* edges and proteins in different species through a *orthologous-to* edge. We then apply a method to generate knowledge graph embeddings [4] to this graph and generate a vector representation for each protein. Furthermore, we integrate this vector representation with the protein sequence representation in our model, resulting in a multi-modal model that utilizes both protein sequences and protein interactions. Incorporating this network information significantly improves the performance for almost all GO classes, and the overall performance of our DeepGO method improves significantly in comparison with DeepGOSeq which uses only protein sequence as a feature, and in comparison to the BLAST baseline. Table 1 summarizes the results.

We find that the predictive performance of our model varies significantly between proteins in different organisms, in particular between single-cell and multi-cellular organisms. Table 2 summarizes the performance we achieve for individual organisms, and further broadly distinguishes between eukaryotic and prokaryotic organisms. We find that DeepGO achieves high performance for well-characterized model organisms, likely due to the rich characterization of protein functions in these organisms; other organisms do not have a large set of manually asserted function annotations and are therefore represented more sparsely in our evaluation set.

We further evaluated how well DeepGO performs on different types of proteins. InterPro classifies proteins into families, domains and important sites [13]. We evaluate DeepGO’s performance by grouping proteins by their InterPro annotations. Supplementary Table 1 shows the performance for InterPro classes with at least 50 protein annotations in our test set. We find that for some important protein families, such as p53-like transcription factors (IPR008967), DeepGO can achieve high performance in all three GO ontologies, while for other kinds of proteins, such as those with a Ubiquitin-related domain (IPR029071), DeepGO fails to predict annotations to BP and MF accurately.

We further perform a term-centric evaluation [22] in which we test how accurate our predictions are for different GO functions. Supplementary Table 2 shows the best performing GO functions from each ontology. Unsurprisingly, high-level functions with a large number of annotations generally perform significantly better than more specific functions. We further test whether the variance in predictive performance is intrinsic to our method or the result of different amounts of training data available for proteins of different families, with different domains, or for GO functions with different number of annotations. We plot the predictive performance of DeepGO as a function of the number of training samples in Figure 2, and observe that performance is strongly correlated with the number of training instances. However, due to the hierarchical

nature of GO, an increased number of training instances will always be available for more general, high-level functions. In the future, additional weights based on information content of GO classes [23] should be assigned to more specific functions which contain more information [10, 22]; using these weights during training of our model may improve performance for more specific functions.

Method	BP			MF			CC		
	F_{\max}	AvgPr	AvgRc	F_{\max}	AvgPr	AvgRc	F_{\max}	AvgPr	AvgRc
BLAST	0.31	0.30	0.33	0.37	0.37	0.38	0.36	0.32	0.42
DeepGOSeq	0.25	0.20	0.33	0.36	0.47	0.29	0.57	0.59	0.55
DeepGO	0.36	0.39	0.34	0.46	0.60	0.38	0.63	0.66	0.61
BLAST (selected terms)	0.34	0.38	0.32	0.54	0.61	0.48	0.50	0.51	0.49
DeepGOSeq (selected terms)	0.27	0.20	0.38	0.38	0.47	0.32	0.57	0.61	0.55
DeepGO (selected terms)	0.40	0.45	0.36	0.50	0.62	0.42	0.64	0.66	0.62

Table 1. Overview of our model’s performance and comparison to BLAST baseline. The DeepGOSeq model uses only sequence information, while DeepGO uses both the protein sequence and network interactions as input. The first part of the evaluation shows performance results when considering all GO annotations (even those that our model cannot predict), while the second part focuses on the selected terms for which our model can generate predictions.

Organism	BP			MF			CC		
	F_{\max}	AvgPr	AvgRc	F_{\max}	AvgPr	AvgRc	F_{\max}	AvgPr	AvgRc
Eukaryotes	0.36	0.39	0.34	0.48	0.63	0.39	0.63	0.65	0.62
Human	0.39	0.45	0.34	0.51	0.65	0.42	0.61	0.59	0.63
Mouse	0.37	0.40	0.34	0.49	0.61	0.41	0.60	0.65	0.56
Rat	0.36	0.37	0.35	0.50	0.63	0.42	0.55	0.56	0.54
Fruit Fly	0.36	0.42	0.32	0.50	0.62	0.43	0.57	0.66	0.49
Yeast	0.40	0.48	0.34	0.43	0.49	0.38	0.58	0.62	0.54
Fission Yeast	0.38	0.40	0.37	0.44	0.59	0.34	0.77	0.77	0.77
Zebrafish	0.37	0.45	0.31	0.56	0.59	0.53	0.66	0.65	0.67
Prokaryotes	0.36	0.41	0.32	0.38	0.45	0.33	0.66	0.75	0.60
Ecoli	0.37	0.42	0.32	0.38	0.49	0.31	0.68	0.79	0.60
Mycobacterium tuberculosis	0.37	0.51	0.29	0.39	0.51	0.32	0.69	0.75	0.63
Pseudomonas aeruginosa	0.46	0.57	0.47	0.31	0.32	0.37	0.50	1.00	0.33
Bacillus subtilis	0.38	0.46	0.32	0.43	0.42	0.44	0.43	1.00	0.28

Table 2. Performance of our method distinguished by organisms. We use the DeepGO model that combines both sequence and network information for this prediction.

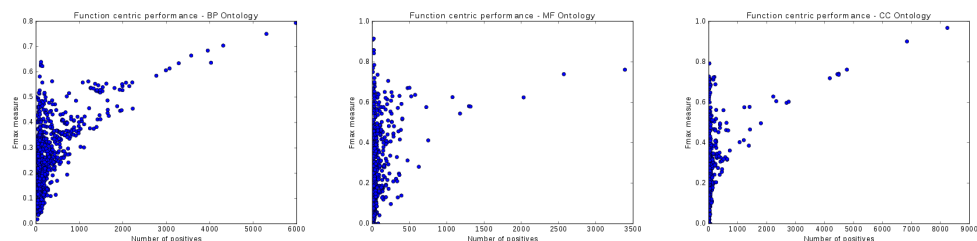


Figure 2. Term centric performance. These plots show the performance of our model for each term in our subset of GO as a function of the number of supporting proteins in test set which are annotated by the term.

4 Discussion

4.1 Multi-modal function prediction

Computational approaches to function prediction have been developed for many years [22]. One of the most basic approaches for function prediction has been the use of BLAST [5] to identify proteins with high sequence similarity and known functions, and assign the functions of the best matching protein to the protein to be characterized. Approaches for orthology-based function prediction include more comprehensive modelling of evolutionary relations, including relations between protein subdomains [14], and these can outperform simple BLAST baseline experiments. Other approaches for function prediction rely on structure prediction. It is well known that protein tertiary structure strongly influences a protein’s functions, but prediction of protein structure remains a challenging computational problem [20], and even with known protein structure, functions cannot always be predicted accurately. Additionally, high-level physiological functions, such as *vocalization behavior* (GO:0071625), will not be predictable from a single protein’s sequence or structure alone but require complex pathways and interacting proteins, all of which contribute to the function.

While many of these approaches rely on hand-crafted features, some approaches already applied feature learning (i.e., deep learning) to parts of these data types. For example, feature learning approaches have significantly improved the prediction of transcription factor binding sites and functional impact of genomic variants [3,30]. Here, we have extended the application of deep learning approaches in function prediction in three ways: first, we apply feature learning through the use of a CNN and embedding layer to learn a representation of protein sequence; second, we developed a deep, ontology-structured classification model that can refine features on each distinction present in the GO; and third, we use multi-modal data sources, in particular the protein structure and information from protein-protein interaction networks, within a single model. Through the multi-modal nature of our machine learning model, other types of data can be integrated within the DeepGO model as long as they can be used as input to a representation learning method that learns vector representations. For example, protein structure information, if available, could be incorporated in our model by adding another feature learning branch that generates dense, low-dimensional representations of protein structure [29] and using these as input to our hierarchical classifier.

4.2 Hierarchical classification on ontologies

In addition to the multi-modal nature of features used in DeepGO, another contribution of our work is the deep hierarchical classification model that optimizes predictive performance on whole hierarchies, accounts for class dependencies, learns features in a hierarchical manner, and is optimized jointly together with the feature learning component of our model in an end-to-end manner. Our method can be applied to other applications with a similarly structured output space and which rely on learning feature representations. In particular, we plan to apply our model for predicting disease associations of genes which are encoded using the Disease Ontology [21], or phenotype associations of genetic variants which are encoded using phenotype ontologies [15].

The advantages of our model are its potential for end-to-end learning, the global optimization, and the potential to predict any class given sufficient training data. In particular the end-to-end learning provides benefits over approaches such as structured support vector machines [25], which generally rely on hand-crafted feature vectors.

However, our model also has disadvantages. First, it needs large amounts of training data for each class; this data is readily available through the manual GO annotations that have been created for many years, but will not easily be available for other areas of

application, such as predicting phenotype annotations or effects of variants. Furthermore, our model is complex and requires large computational resources for training, and therefore may not be applicable in all settings.

In the future, we intend to extend our hierarchical model in several directions. First, we plan to include more information from GO, in particular parthood relations and regulatory relations, which may provide additional information. We will also explore adding more features, such as additional types of interactions (genetic interactions, or co-expression networks), and information extracted from text.

Supplementary materials

InterPro	InterPro Name	BP			MF			CC		
		F _{max}	AvgPr	AvgRc	F _{max}	AvgPr	AvgRc	F _{max}	AvgPr	AvgRc
IPR008967	p53-like transcription factor, DNA-binding	0.44	0.48	0.40	0.63	0.65	0.61	0.80	0.78	0.81
IPR013083	Zinc finger, RING/FYVE/PHD-type	0.37	0.38	0.36	0.50	0.57	0.45	0.67	0.66	0.68
IPR017907	Zinc finger, RING-type, conserved site	0.26	0.33	0.22	0.39	0.61	0.28	0.57	0.54	0.60
IPR013087	Zinc finger C2H2-type	0.47	0.44	0.51	0.58	0.53	0.64	0.77	0.75	0.79
IPR011991	Winged helix-turn-helix DNA-binding domain	0.39	0.41	0.37	0.41	0.52	0.34	0.64	0.65	0.64
IPR015943	WD40/YVTN repeat-like-containing domain	0.41	0.41	0.40	0.52	0.62	0.45	0.66	0.66	0.65
IPR019775	WD40 repeat, conserved site	0.40	0.39	0.41	0.55	0.60	0.50	0.67	0.67	0.68
IPR001680	WD40 repeat	0.41	0.41	0.40	0.53	0.60	0.48	0.67	0.68	0.67
IPR029071	Ubiquitin-related domain	0.28	0.28	0.28	0.48	0.54	0.43	0.63	0.67	0.61
IPR016135	Ubiquitin-conjugating enzyme/RWD-like	0.42	0.39	0.44	0.57	0.58	0.57	0.65	0.62	0.69
IPR023313	Ubiquitin-conjugating enzyme, active site	0.42	0.39	0.46	0.59	0.57	0.61	0.65	0.59	0.71
IPR018200	Ubiquitin specific protease, conserved site	0.31	0.32	0.31	0.46	0.53	0.40	0.67	0.67	0.67
IPR028889	Ubiquitin specific protease domain	0.32	0.32	0.31	0.46	0.53	0.40	0.67	0.67	0.67
IPR012336	Thioredoxin-like fold	0.26	0.28	0.25	0.48	0.50	0.47	0.66	0.64	0.68
IPR000727	Target SNARE coiled-coil homology domain	0.44	0.46	0.42	0.56	0.81	0.43	0.53	0.73	0.41
IPR008271	Serine/threonine-protein kinase, active site	0.41	0.42	0.40	0.63	0.70	0.57	0.59	0.61	0.58
IPR001452	SH3 domain	0.35	0.40	0.31	0.44	0.55	0.36	0.55	0.56	0.54
IPR000980	SH2 domain	0.40	0.43	0.37	0.53	0.66	0.44	0.65	0.66	0.65
IPR029063	S-adenosyl-L-methionine-dependent methyltransferase	0.43	0.43	0.43	0.43	0.57	0.35	0.73	0.71	0.75
IPR000504	RNA recognition motif domain	0.45	0.46	0.45	0.70	0.66	0.74	0.69	0.66	0.72
IPR011009	Protein kinase-like domain	0.39	0.42	0.36	0.61	0.67	0.56	0.59	0.61	0.57
IPR017441	Protein kinase, ATP binding site	0.41	0.45	0.38	0.64	0.70	0.60	0.57	0.59	0.56
IPR011993	PH domain-like	0.38	0.42	0.34	0.45	0.61	0.36	0.55	0.54	0.57
IPR027417	P-loop containing nucleoside triphosphate hydrolase	0.37	0.40	0.34	0.37	0.60	0.27	0.63	0.66	0.61
IPR016040	NAD(P)-binding domain	0.37	0.39	0.35	0.40	0.59	0.30	0.73	0.70	0.75
IPR020846	Major facilitator superfamily domain	0.44	0.47	0.41	0.43	0.65	0.32	0.61	0.66	0.57
IPR032675	Leucine-rich repeat domain, L domain-like	0.32	0.45	0.25	0.47	0.70	0.36	0.48	0.55	0.43
IPR013783	Immunoglobulin-like fold	0.33	0.36	0.31	0.44	0.61	0.34	0.49	0.53	0.46
IPR009057	Homeobox domain-like	0.39	0.44	0.35	0.57	0.64	0.52	0.75	0.74	0.75
IPR009071	High mobility group box domain	0.40	0.41	0.38	0.64	0.62	0.66	0.74	0.72	0.75
IPR011992	EF-hand domain pair	0.35	0.45	0.28	0.53	0.62	0.46	0.63	0.70	0.57
IPR013320	Concanavalin A-like lectin/glucanase domain	0.26	0.34	0.21	0.35	0.60	0.25	0.57	0.56	0.57
IPR000008	C2 domain	0.33	0.39	0.29	0.38	0.54	0.29	0.50	0.69	0.39

Table 1. Performance of DeepGO by InterPro domains. Only InterPro domains for which at least 50 proteins are in our evaluation dataset are included in this evaluation.

Function	Label	DeepGO		DeepGOSeq	
		F _{max}	ROC AUC	F _{max}	ROC AUC
Biological Process					
GO:0009987	cellular process	0.793545	0.680064	0.793765	0.540680
GO:0044699	single-organism process	0.750229	0.699637	0.738709	0.577044
GO:0065007	biological regulation	0.704066	0.759365	0.677123	0.689570
GO:0008152	metabolic process	0.634190	0.759272	0.544373	0.608695
GO:0032502	developmental process	0.551414	0.620468	0.392551	0.625560
GO:0050896	response to stimulus	0.454906	0.683399	0.393794	0.512953
GO:0071840	cellular component organization or biogenesis	0.448368	0.703925	0.365183	0.572168
GO:0051179	localization	0.426162	0.708099	0.311107	0.489611
GO:0032501	multicellular organismal process	0.413983	0.531594	0.223127	0.566755
GO:0040007	growth	0.403571	0.237761	0.074300	0.326924
GO:0002376	immune system process	0.383117	0.337897	0.085541	0.393173
GO:0022414	reproductive process	0.370014	0.434946	0.190107	0.566350
GO:0051704	multi-organism process	0.277030	0.512176	0.169651	0.537286
GO:0007610	behavior	0.262774	0.217460	0.049016	0.405271
GO:0040011	locomotion	0.200238	0.415350	0.071258	0.537358
GO:0022610	biological adhesion	0.153846	0.145779	0.042748	0.187945
GO:0023052	signaling	0.150171	0.084057	0.017836	0.010441
GO:0048511	rhythmic process	0.116883	0.057025	0.015441	0.027048
GO:0000003	reproduction	0.072398	0.010535	0.013423	0.002335
Molecular Function					
GO:0005488	binding	0.760884	0.778792	0.726436	0.714915
GO:0003824	catalytic activity	0.738823	0.835322	0.671065	0.732225
GO:0005215	transporter activity	0.636451	0.314824	0.594164	0.450674
GO:0001071	nucleic acid binding transcription factor activity	0.519453	0.362382	0.388293	0.448391
GO:0060089	molecular transducer activity	0.502392	0.350086	0.342723	0.384180
GO:0004871	signal transducer activity	0.481572	0.378499	0.343465	0.496081
GO:0098772	molecular function regulator	0.329268	0.334650	0.179612	0.576424
GO:0016209	antioxidant activity	0.325926	0.062499	0.056395	0.025002
GO:0000988	transcription factor activity, protein binding	0.293413	0.239255	0.176398	0.333591
GO:0005198	structural molecule activity	0.242152	0.277404	0.058824	0.426995
GO:0009055	electron carrier activity	0.187500	0.017467	0.027778	0.040924
GO:0045182	translation regulator activity	0.070175	0.032282	0.007722	0.027473
Cellular Component					
GO:0044464	cell part	0.967330	0.826043	0.966631	0.697060
GO:0043226	organelle	0.761161	0.595503	0.708719	0.645590
GO:0016020	membrane	0.605258	0.691536	0.500599	0.710984
GO:0044422	organelle part	0.602635	0.630250	0.495917	0.630139
GO:0044421	extracellular region part	0.498270	0.306901	0.165513	0.575960
GO:0032991	macromolecular complex	0.465488	0.653815	0.335831	0.638300
GO:0005576	extracellular region	0.452276	0.248848	0.368515	0.542654
GO:0044425	membrane part	0.402873	0.505403	0.301491	0.580220
GO:0044456	synapse part	0.371429	0.084840	0.020779	0.004898
GO:0099512	supramolecular fiber	0.345946	0.098424	0.078240	0.021825
GO:0045202	synapse	0.309524	0.032163	0.000000	0.000000
GO:0031974	membrane-enclosed lumen	0.303226	0.199096	0.044743	0.202145
GO:0031012	extracellular matrix	0.291971	0.098603	0.012712	0.014834
GO:0030054	cell junction	0.242424	0.243079	0.062822	0.305787
GO:0009295	nucleoid	0.200000	0.003091	0.000000	0.000000
GO:0044420	extracellular matrix component	0.125000	0.001101	0.000000	0.000000
GO:0044217	other organism part	0.111940	0.047736	0.027149	0.004069
GO:0005623	cell	0.068966	0.022208	0.018182	0.000568
GO:0044423	virion part	0.066158	0.039468	0.000000	0.000000
GO:0019012	virion	0.029412	0.019432	0.000000	0.000000

Table 2. Performance of DeepGO distinguished by GO functions.

Acknowledgements

We acknowledge use of the compute resources of the Computational Bioscience Research Center (CBRC) at King Abdullah University of Science and Technology (KAUST).

Funding

This work was supported by funding from King Abdullah University of Science and Technology (KAUST) [FCC/1/1976-08-01].

References

1. M. Abadi, P. Barham, J. Chen, Z. Chen, A. Davis, J. Dean, M. Devin, S. Ghemawat, G. Irving, M. Isard, M. Kudlur, J. Levenberg, R. Monga, S. Moore, D. G. Murray, B. Steiner, P. Tucker, V. Vasudevan, P. Warden, M. Wicke, Y. Yu, and X. Zheng. Tensorflow: A system for large-scale machine learning. In *Proceedings of the 12th USENIX Conference on Operating Systems Design and Implementation, OSDI'16*, pages 265–283, Berkeley, CA, USA, 2016. USENIX Association.
2. B. Alberts et al. *Molecular Biology of the Cell, Fourth Edition*. Garland Science, 4 edition, 2002.
3. B. Alipanahi, A. Delong, M. T. Weirauch, and B. J. Frey. Predicting the sequence specificities of DNA- and RNA-binding proteins by deep learning. *Nature biotechnology*, 33(8):831–838, Aug. 2015.
4. M. Alshahrani, M. A. Khan, O. Maddouri, A. R. Kinjo, N. Queralt-Rosinach, and R. Hoehndorf. Neuro-symbolic representation learning on biological knowledge graphs. *Bioinformatics*, 2017. advance access.
5. S. F. Altschul, T. L. Madden, A. A. Schäffer, J. Zhang, Z. Zhang, W. Miller, and D. J. Lipman. Gapped BLAST and PSI-BLAST: a new generation of protein database search programs. *Nucleic acids research*, 25(17):3389–3402, Sept. 1997.
6. M. Ashburner, C. A. Ball, J. A. Blake, D. Botstein, H. Butler, M. J. Cherry, A. P. Davis, K. Dolinski, S. S. Dwight, J. T. Eppig, M. A. Harris, D. P. Hill, L. I. Tarver, A. Kasarskis, S. Lewis, J. C. Matese, J. E. Richardson, M. Ringwald, G. M. Rubin, and G. Sherlock. Gene ontology: tool for the unification of biology. *Nature Genetics*, 25(1):25–29, May 2000.
7. Y. Bengio, R. Ducharme, P. Vincent, and C. Jauvin. A neural probabilistic language model. *journal of machine learning research*, 3(Feb):1137–1155, 2003.
8. Y. Bengio and Y. Lecun. Convolutional networks for images, speech, and time-series, 1995.
9. E. Boutet et al. *UniProtKB/Swiss-Prot, the Manually Annotated Section of the UniProt KnowledgeBase: How to Use the Entry View*, pages 23–54. Springer New York, New York, NY, 2016.
10. W. T. Clark and P. Radivojac. Information-theoretic evaluation of predicted ontological annotations. *Bioinformatics*, 29(13):i53, 2013.

-
11. R. Collobert, J. Weston, L. Bottou, M. Karlen, K. Kavukcuoglu, and P. Kuksa. Natural language processing (almost) from scratch. *Journal of Machine Learning Research*, 12(Aug):2493–2537, 2011.
 12. M. Costanzo, B. VanderSluis, E. N. Koch, A. Baryshnikova, C. Pons, G. Tan, W. Wang, M. Usaj, J. Hanchard, S. D. Lee, V. Pelechano, E. B. Styles, M. Billmann, J. van Leeuwen, N. van Dyk, Z.-Y. Lin, E. Kuzmin, J. Nelson, J. S. Piotrowski, T. Srikumar, S. Bahr, Y. Chen, R. Deshpande, C. F. Kurat, S. C. Li, Z. Li, M. M. Usaj, H. Okada, N. Pascoe, B.-J. San Luis, S. Sharifpoor, E. Shuteriqi, S. W. Simpkins, J. Snider, H. G. Suresh, Y. Tan, H. Zhu, N. Malod-Dognin, V. Janjic, N. Przulj, O. G. Troyanskaya, I. Stagljar, T. Xia, Y. Ohya, A.-C. Gingras, B. Raught, M. Boutros, L. M. Steinmetz, C. L. Moore, A. P. Rosebrock, A. A. Caudy, C. L. Myers, B. Andrews, and C. Boone. A global genetic interaction network maps a wiring diagram of cellular function. *Science*, 353(6306), 2016.
 13. R. D. Finn, T. K. Attwood, P. C. Babbitt, A. Bateman, P. Bork, A. J. Bridge, H.-Y. Chang, Z. Dosztányi, S. El-Gebali, M. Fraser, J. Gough, D. Haft, G. L. Holliday, H. Huang, X. Huang, I. Letunic, R. Lopez, S. Lu, A. Marchler-Bauer, H. Mi, J. Mistry, D. A. Natale, M. Necci, G. Nuka, C. A. Orengo, Y. Park, S. Pesseat, D. Piovesan, S. C. Potter, N. D. Rawlings, N. Redaschi, L. Richardson, C. Rivoire, A. Sangrador-Vegas, C. Sigrist, I. Sillitoe, B. Smithers, S. Squizzato, G. Sutton, N. Thanki, P. D. Thomas, S. Tosatto, C. H. Wu, I. Xenarios, L.-S. Yeh, S.-Y. Young, and A. L. Mitchell. Interpro in 2017—beyond protein family and domain annotations. *Nucleic Acids Research*, 45(D1):D190, 2017.
 14. P. Gaudet, M. S. Livstone, S. E. Lewis, and P. D. Thomas. Phylogenetic-based propagation of functional annotations within the gene ontology consortium. *Briefings in Bioinformatics*, 12(5):449, 2011.
 15. G. V. Gkoutos, P. N. Schofield, and R. Hoehndorf. The anatomy of phenotype ontologies: principles, properties and applications. *Briefings in Bioinformatics*, 2017.
 16. X. Glorot and Y. Bengio. Understanding the difficulty of training deep feedforward neural networks. In *Aistats*, volume 9, pages 249–256, 2010.
 17. G. E. Hinton. Learning distributed representations of concepts. In *Proceedings of the eighth annual conference of the cognitive science society*, volume 1, page 12. Amherst, MA, 1986.
 18. J. Huerta-Cepas, D. Szklarczyk, K. Forslund, H. Cook, D. Heller, M. C. Walter, T. Rattei, D. R. Mende, S. Sunagawa, M. Kuhn, L. J. Jensen, C. von Mering, and P. Bork. egglog 4.5: a hierarchical orthology framework with improved functional annotations for eukaryotic, prokaryotic and viral sequences. *Nucleic Acids Research*, 44(D1):D286, 2016.
 19. J. Konc, M. Hodošček, M. Ogrizek, J. Trykowska Konc, and D. Janežič. Structure-based function prediction of uncharacterized protein using binding sites comparison. *PLOS Computational Biology*, 9(11):1–9, 11 2013.
 20. J. Moult, K. Fidelis, A. Kryshafovich, T. Schwede, and A. Tramontano. Critical assessment of methods of protein structure prediction (casp) — round x. *Proteins: Structure, Function, and Bioinformatics*, 82:1–6, 2014.

-
21. J. Osborne, J. Flatow, M. Holko, S. Lin, W. Kibbe, L. Zhu, M. Danila, G. Feng, and R. Chisholm. Annotating the human genome with disease ontology. *BMC Genomics*, 10(Suppl 1):S6+, 2009.
 22. P. Radivojac, W. T. Clark, T. R. Oron, A. M. Schnoes, T. Wittkop, A. Sokolov, K. Graim, C. Funk, K. Verspoor, A. Ben-Hur, G. Pandey, J. M. Yunes, A. S. Talwalkar, S. Repo, M. L. Souza, D. Piovesan, R. Casadio, Z. Wang, J. Cheng, H. Fang, J. Gough, P. Koskinen, P. Toronen, J. Nokso-Koivisto, L. Holm, D. Cozzetto, D. W. A. Buchan, K. Bryson, D. T. Jones, B. Limaye, H. Inamdar, A. Datta, S. K. Manjari, R. Joshi, M. Chitale, D. Kihara, A. M. Lisewski, S. Erdin, E. Venner, O. Lichtarge, R. Rentzsch, H. Yang, A. E. Romero, P. Bhat, A. Paccanaro, T. Hamp, R. Kaszner, S. Seemayer, E. Vicedo, C. Schaefer, D. Achten, F. Auer, A. Boehm, T. Braun, M. Hecht, M. Heron, P. Honigschmid, T. A. Hopf, S. Kaufmann, M. Kiening, D. Krompass, C. Landerer, Y. Mahlich, M. Roos, J. Bjerne, T. Salakoski, A. Wong, H. Shatkay, F. Gatzmann, I. Sommer, M. N. Wass, M. J. E. Sternberg, N. Skunca, F. Supek, M. Bosnjak, P. Panov, S. Dzeroski, T. Smuc, Y. A. I. Kourmpetis, A. D. J. van Dijk, C. J. F. t. Braak, Y. Zhou, Q. Gong, X. Dong, W. Tian, M. Falda, P. Fontana, E. Lavezzo, B. Di Camillo, S. Toppo, L. Lan, N. Djuric, Y. Guo, S. Vucetic, A. Bairoch, M. Linial, P. C. Babbitt, S. E. Brenner, C. Orengo, B. Rost, S. D. Mooney, and I. Friedberg. A large-scale evaluation of computational protein function prediction. *Nat Meth*, 10(3):221–227, Jan. 2013.
 23. P. Resnik. Semantic similarity in a taxonomy: An Information-Based measure and its application to problems of ambiguity in natural language. *Journal of Artificial Intelligence Research*, 11:95–130, 1999.
 24. R. Sharan, I. Ulitsky, and R. Shamir. Network-based prediction of protein function. *Molecular Systems Biology*, 3(1), 2007.
 25. A. Sokolov and A. Ben-Hur. Hierarchical classification of gene ontology terms using the gostruct method. *J. Bioinformatics and Computational Biology*, 8(2):357–376, 2010.
 26. D. Szklarczyk, A. Franceschini, S. Wyder, K. Forslund, D. Heller, J. Huerta-Cepas, M. Simonovic, A. Roth, A. Santos, K. P. Tsafou, M. Kuhn, P. Bork, L. J. Jensen, and C. von Mering. String v10: protein–protein interaction networks, integrated over the tree of life. *Nucleic Acids Research*, 43(D1):D447, 2015.
 27. T. Tieleman and G. Hinton. Lecture 6.5—RmsProp: Divide the gradient by a running average of its recent magnitude. COURSERA: Neural Networks for Machine Learning, 2012.
 28. K. M. Verspoor. *Roles for Text Mining in Protein Function Prediction*, pages 95–108. Springer New York, New York, NY, 2014.
 29. S. Wang, S. Sun, Z. Li, R. Zhang, and J. Xu. Accurate de novo prediction of protein contact map by ultra-deep learning model. *PLOS Computational Biology*, 13(1):1–34, 01 2017.
 30. J. Zhou and O. G. Troyanskaya. Predicting effects of noncoding variants with deep learning-based sequence model. *Nature Methods*, 12(10):931–934, Aug. 2015.